statistics are larger than those for the copolymers prepared with the δ-TiCl$_3$/Et$_2$AlCl system. Furthermore, a two-site mechanism, in which one site (P-site) polymerizes propylene predominantly and the other site (E-site) polymerizes ethylene predominantly, is confirmed in the catalytic systems used for Kakugo's and Doi's copolymers. In the catalytic system for Doi's copolymers, the P-site produces random or moderately alternating copolymer and the E-site produces block copolymers containing long ethylene sequences. The applicability of model MM is verified by the analyses of Cozewith's copolymers prepared with various titanium-based catalytic systems. Therefore, it is concluded on the basis of the sequence distributions determined by ^{13}C NMR spectra that model MM is appropriate to describe the ethylene-propylene copolymerization mechanism with heterogeneous Ziegler-Natta catalytic systems, as far as it is concerned with the analyzed sequence distribution data of E-P copolymers in this study.

Acknowledgment. T. H. thanks Tokuyama Soda Co. Ltd. for granting him a leave from the company to develop this study at Tokyo Institute of Technology.

Registry No. E, 74-85-1; P, 115-07-1; (E)(P) (copolymer), 9010-79-1.

References and Notes

(1) Wilkes, C. E.; Carman, C. J.; Harrington, R. A. *J. Polym. Sci., Polym. Symp.* **1973**, *43*, 237.
(2) Ray, G. J.; Johnson, P. E.; Knox, J. R. *Macromolecules* **1977**, *10*, 773.
(3) Randall, J. C. *Macromolecules* **1978**, *11*, 33.
(4) Smith, W. V. *J. Polym. Sci., Polym. Phys. Ed.* **1980**, *18*, 1573, 1587.
(5) Kakugo, M.; Naito, Y.; Mizunuma, K.; Miyatke, T. *Macromolecules* **1982**, *15*, 1150.
(6) Cheng, H. N. *Macromolecules* **1984**, *17*, 1950.
(7) Doi, Y.; Ohnishi, R.; Soga, K. *Makromol. Chem., Rapid Commun.* **1983**, *4*, 169.
(8) Soga, K.; Shiono, T.; Doi, Y. *Polym. Bull. (Berlin)* **1983**, *10*, 168.
(9) Cheng, H. N. *Anal. Chem.* **1982**, *54*, 1828.
(10) Ross, J. F. *J. Macromol. Sci., Chem.* **1984**, *A21*(4), 453.
(11) Ross, J. F. Presented at the International Symposium on Transition Metal Catalyzed Polymerization, Akron, OH, June 16, 1986; paper 60.
(12) Ross, J. F. *J. Macromol. Sci., Chem.* **1987**, *A24*(2), 211.
(13) Cozewith, C. *Macromolecules* **1987**, *20*, 1237.
(14) Zhu, S. N.; Yang, X. Z.; Chûjô, R. *Polym. J. (Tokyo)* **1983**, *15*, 859.
(15) Inoue, Y.; Itabashi, Y.; Chûjô, R.; Doi, Y. *Polymer* **1984**, *25*, 1640.
(16) Hayashi, T.; Inoue, Y.; Chûjô, R.; Asakura, T. *Polymer* **1988**, *29*, 138.
(17) Asakura, T.; Nishiyama, Y.; Doi, Y. *Macromolecules* **1987**, *20*, 616.
(18) Zambelli, A.; Locatelli, P.; Bajo, G. *Macromolecules* **1977**, *10*, 773.
(19) Soga, K.; Ohnishi, R.; Sano, T. *Polym. Bull. (Berlin)* **1982**, *7*, 547.
(20) Randall, J. C. *J. Polym. Sci., Polym. Phys. Ed.* **1976**, *14*, 1693.
(21) Marquardt, D. W. *J. Soc. Ind. Appl. Math.* **1963**, *11*, 431.
(22) Kissin, Y. V. *Isospecific Polymerization of Olefins*; Springer-Verlag: New York, 1985; Chapter II.
(23) Soga, K.; Sano, T.; Ohnishi, R. *Polym. Bull. (Berlin)* **1981**, *4*, 157.
(24) Randall, J. C. *J. Polym. Sci., Polym. Phys. Ed.* **1976**, *14*, 2083.
(25) Lukach, C. A.; Spurlin, H. M. *Copolymerization*; Ham, G. E., Ed.; Interscience: New York, 1964.

Three-Dimensional Structure of Main-Chain Liquid-Crystalline Copolymers. 1. Cylindrically Averaged Intensity Transforms of Single Chains

Amit Biswas and John Blackwell*

Department of Macromolecular Science, Case Western Reserve University,
Cleveland, Ohio 44106-2699. Received October 16, 1987

ABSTRACT: As a first step in our X-ray analysis of the three-dimensional structure of wholly aromatic main-chain liquid-crystalline copolyesters, this paper describes calculation of the cylindrically averaged transforms of single chains. Attention is focused on the copolyesters prepared from *p*-hydroxybenzoic acid (HBA) of 2-hydroxy-6-naphthoic acid (HNA). Previous analyses of the aperiodic meridional intensity distribution have shown that these copolymers consist of arrays of parallel chains of completely random comonomer sequence. Nevertheless, the X-ray fiber diagrams contain equatorial and off-equatorial Bragg maxima, which point to the existence of three-dimensional order. The cylindrically averaged transforms are calculated by an extension of the one-dimensional model used previously, when the chain is treated as a one-dimensional paracrystal with random coordination statistics for the two monomers. It is found that a dimer repeat must be assumed in order to generate the intense layer line that occurs between the equator and the first meridional maximum. The chain is treated as a random array of the four possible dimers with a fixed conformation but with limited conformational correlation between successive dimer units. Good agreement is obtained when the dimers have conformations analogous to those of poly(*p*-benzamide) and poly(*p*-phenyleneterephthalamide), and analysis of the chain packing is necessary to decide between the various possibilities.

Introduction

The solid-state structure of liquid-crystalline polymers has stimulated much interest and research in recent years.[1-3] In particular, there has been extensive study of a group of wholly aromatic random copolyesters, which are thermotropic main-chain liquid-crystalline polymers with applications as high-strength fibers and high-performance moldings. The bulk properties of these copolymers show a high sensitivity to relatively small changes in the chemical structure and proportions of the monomer components.[4] In addition, the excellent mechanical properties of these systems appear to correlate with the development of three-dimensional crystalline order, which develops on cooling after processing from the melt and which increases on thermal treatment.[5]

Previous papers from this laboratory have described X-ray analyses of the structure of wholly aromatic thermotropic copolyesters and also of an analogous lyotropic

0024-9297/88/2221-3146$01.50/0

copolyamide.[6-9] This work has concentrated on derivation of a model for the individual copolymer chain, based on the interpretation of the diffracted intensity along the meridian of the X-ray fiber diagrams. Some of the systems that have been studied are listed below.

HBA/HNA [10]

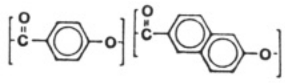

HBA/DHN/TPA [11]

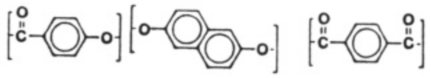

HBA/BP/TPA [12]

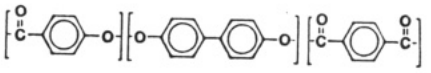

PDA/TPA/DPE [13]

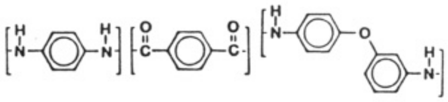

HBA, *p*-hydroxybenzoic acid
HNA, 2-hydroxy-6-naphthoic acid
DHN, 2,6-dihydroxynaphthalene
DPE, 3-aminophenyl 4-aminophenyl ether
TPA, terephthalic acid
BP, biphenol
PDA, phenylenediamine

Figure 1 shows the diffraction patterns from melt-drawn fibers of the HBA/HNA copolymer for a 30/70 mole ratio. Most of the diffracted intensity lies on the meridian and on the equator of the X-ray pattern, and the latter region is by far the more intense. The meridional maxima are found to be aperiodic; i.e., they are not orders of a simple repeat and vary steadily in *d*-spacing with HBA/HNA monomer ratio across the entire composition range. We have shown that the position and intensities of these maxima are consistent with a structure comprised of a parallel array of highly extended chains with completely random monomer sequences.[14] These conclusions were based on modeling the chains as a one-dimensional paracrystal with random coordination statistics for the two monomers. Introduction of nonrandomness into the model chain led to significant deviations in the positions of the calculated meridional maxima from the observed values. We concluded therefore that all but minimal blockiness can be ruled out.[15]

We now wish to consider the three-dimensional packing of the chains, information on which is derived from the complete scattering pattern. In the case of as-spun fibers of the three copolyesters mentioned above, Bragg maxima are seen on the equator at $d = 4.6$, 2.6, and 2.3 Å, which are indexed as the 100, 110, and 200 reflections for a hexagonal unit cell with $a = 5.2$ Å. In addition, an off-equatorial maximum is observed at $d = 3.3$ Å, which points to the presence of some three-dimensional order. There is evidence that annealing leads to a significant increase in the intensities of the equatorial and off-equatorial maxima, suggesting an increase in the three-dimensional order.[5] In certain copolyester systems, the existence of polymorphic structures on annealing has also been reported.[9]

In order to determine the three-dimensional structure in the solid state, we need to consider the possible ways in which order can be developed in random copolymers. Windle and co-workers[16] have used electron and optical microscopy along with X-ray data to study the orientation and conformation of the chains of the HBA/HNA copolymer in the solid state. They propose a biaxial nematic structure arising out of the formation of nonperiodic lattice (npl) crystals, which consist of short identical copolymer sequences in parallel alignment. On the other hand, Wendorff and co-workers[17] have postulated on the formation of imperfect microcrystals in the solid state on the basis of X-ray, volumetric, and calorimetric data. There have been other notable studies on the solid-state structure of these rigid chain systems by DSC, NMR, and dynamic mechanical measurements.[18-20]

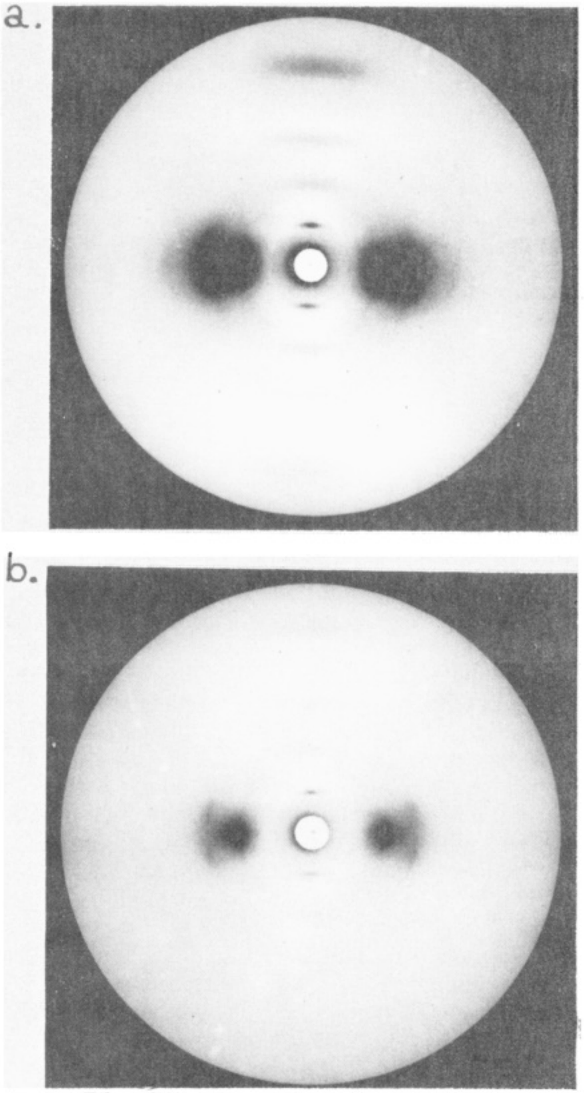

Figure 1. Fiber diffraction patterns from melt-drawn samples of 30/70 copoly(HBA/HNA) at high and low exposures. The fiber axis is vertical.

The present paper describes calculation of the cylindrically averaged intensity transforms of a single chain of random sequences of the HBA/HNA copolymer as a step toward determining the three-dimensional structure. The approach of Chivers et al.[21] for calculating the cylindrically averaged transforms has been streamlined and generalized for multicomponent copolymers. Thereafter, the effects of chain conformation on the intensity transforms have been studied. The theoretical approach and the results are described below.

Cylindrically Averaged Intensity Transforms

The intensity from a three-dimensional arrangement of N atoms in space is given by

$$I(X,Y,Z) = F(X,Y,Z)\, F^*(X,Y,Z) \qquad (1)$$

where

$$F(X,Y,Z) = \sum_{j=1}^{N} f_j \exp[2\pi i(Xx_j + Yy_j + Zz_j)] \quad (2)$$

and * denotes the complex conjugate. f_j is the atomic scattering factor of the jth atom having coordinates x_j, y_j, z_j, and X, Y, Z are the reciprocal space coordinates. In the case of fiber symmetry, it is convenient to express $F(X,Y,Z)$ in cylindrical polar coordinates, whereupon eq 2 can be rewritten

$$F(R,\Phi,Z) = \sum_{j=1}^{N} f_j \exp[2\pi i(r_j R \cos(\Phi - \phi_j) + Zz_j)] \quad (3)$$

where r_j, ϕ_j, z_j and R, Φ, Z are the real space atomic coordinates and reciprocal space coordinates, respectively. For fiber symmetry, there will be cylindrical averaging of $I(R,\Phi,Z)$, and the fiber diagram is a representation of the two-dimensional intensity, $I(R,Z)$.

In our previous papers, we have shown that the positions and approximate intensities of the aperiodic maxima are predicted for an array of parallel extended copolymer chains of completely random comonomer sequence. A model of a short segment of a chain of copoly(HBA/HNA) with a typical random sequence is shown in Figure 2. The planar aromatic and ester groups along with the 1,4 and 2,6 aromatic linkages lead to a relatively straight chain. Consequently, the axial advance per residue is approximately independent of the torsion angles between the aromatic and ester groups. The theoretical meridional intensity, $I(0,Z)$, is derived by considering the projection of the structure on the chain (z) axis and is thus approximately independent of the chain conformation.

However, when we consider the entire diffraction pattern, i.e., $I(R,Z)$, then the actual chain conformation becomes important. Chivers and Blackwell[21] have derived equations for the diffracted intensity from copolymer chains at two extremes of the possible conformation.

The first is an extended random conformation for which there is a completely random set of torsion angles between the planar aromatic and ester groups in the chain. This corresponds approximately to cylindrically averaging each monomer residue independently in real space, as is shown schematically in Figure 3a. The resulting chain would have a cylindrical cross section with no rotational correlation between adjacent monomers and would be expected to pack in an hexagonal array, as is indicated by the equatorial data for the as-spun fibers. The intensity distribution from such a chain is given by

$$I(R,Z) = \sum_{A}\sum_{B}\sum_{l} Q_{AB}(z_l)[A_{AB}(R,Z)\cos(2\pi Z z_l) + B_{AB}(R,Z)\sin(2\pi Z z_l)] \quad (4)$$

where

$$A_{AB}(R,Z) = \sum_{j}\sum_{k} f_{A,j} f_{B,k} J_0(2\pi R r_{A,j}) J_0(2\pi R r_{B,k}) \cos[2\pi Z(z_{B,k} - z_{A,j})] \quad (5)$$

$B_{AB}(R,Z)$ is the equivalent sine term. $Q_{AB}(z_l)$ defines the probability of a comonomer sequence of length z_l starting with monomer A and ending with monomer B. The subscripts A,j and B,k denote the jth atom of monomer A and the kth atom of monomer B. J_0 is the zeroth-order Bessel function for the argument specified.

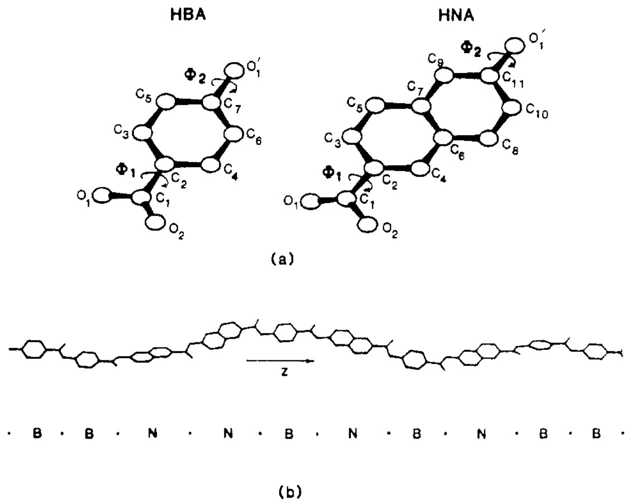

Figure 2. (a) Projections of the model structures of the monomers HBA and HNA. Φ_1 and Φ_2 are the ester–aromatic and aromatic–ester torsion angles, respectively. (b) A model of a short segment of a chain of copoly(HBA/HNA) with a typical random sequence.

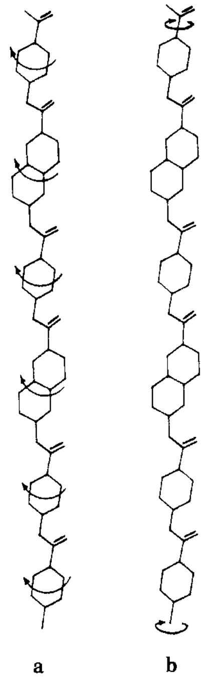

Figure 3. (a) Schematic representation of cylindrical averaging of monomers for an extended random conformation model of the copolymer chain. (b) Schematic representation of cylindrical averaging of the entire chain leading to the extended rigid conformation model.

The second conformation is an extended rigid conformation with specific torsion angles repeated along the chain. In the example shown in Figure 3b, the aromatic–ester and ester–aromatic torsion angles were set at +30° and −30°, respectively, leading to a ribbonlike chain conformation in which the planes of the aromatic groups are all parallel to one another. In this case, $I(R,Z)$ is derived by cylindrical averaging of the full three-dimensional intensity transform $I(R,\Phi,Z)$; i.e., the cylindrical averaging is done in reciprocal space. $I(R,Z)$ has the same form as eq 4 except that $A_{AB}(R,Z)$ and $B_{AB}(R,Z)$ are defined as sums over nth-order Bessel functions of the first kind

$$A_{AB}(R,Z) = \sum_{n}\sum_{j}\sum_{k} f_{A,j} f_{B,k} J_n(2\pi R r_{A,j}) J_n(2\pi R r_{B,k}) \times \cos[n(\phi_{A,j} - \phi_{B,k}) + 2\pi Z(z_{A,j} - z_{B,k})] \quad (6)$$

$B_{AB}(R,Z)$ is the equivalent sine term.

The above calculations can be simplified by modeling the chain as a one-dimensional paracrystalline lattice with random coordination statistics for the constituent polyatomic monomers.[22] Following our previous treatment of the one-dimensional case,[15] the meridional intensity distribution for an infinite chain is written as

$$I(Z) = \sum_{A} p_A F_{AA}(Z) + 2\,\mathrm{Re} \sum_{A}\sum_{B} F_{AB}(Z)\, T_{AB}(Z) \quad (7)$$

where $T_{AB}(Z)$ represents an element of the matrix **T**, defined as

$$\mathbf{T} = \mathbf{P}\frac{\mathbf{M}\cdot\mathbf{X}(Z)}{\mathbf{I} - \mathbf{M}\cdot\mathbf{X}(Z)} \quad (8)$$

I is a unit matrix, and the matrices **P**, **M**, and **X** define the monomer composition, combination probability, and the phase effects associated with the different monomer lengths, respectively. For the HBA/HNA copolymer, the matrices **P**, **M**, and **X** are

$$\mathbf{P} = \begin{bmatrix} P_B & 0 \\ 0 & P_N \end{bmatrix} \qquad \mathbf{M} = \begin{bmatrix} M_{BB} & M_{BN} & M_{BN} \\ M_{NB} & M_{NB} & M_{NN} \end{bmatrix}$$

$$\mathbf{X} = \begin{bmatrix} X_B & 0 \\ 0 & X_N \end{bmatrix}$$

where the subscripts B and N are further abbreviations of HBA and HNA, respectively. For example, P_B is the molar composition of monomer B, M_{BB} is the combination probability for the dimer BB (and is equal to P_B in the case of a completely random sequence), and X_B is the phase term for monomer B (and is equal to $\exp(2\pi i Z z_B)$).

In the discussion below, it will be convenient to treat the chain of copoly(HBA/HNA) as a random array of four dimers rather than two monomers, which allows a pseudodimer repeat to be imposed on the conformation. In this case the interference effects now originate from the spatial correlations of the four dimers BB, BN, NB, and NN, and the matrices **P**, **M**, and **X** are defined as

$$\mathbf{P} = \begin{bmatrix} P_{BB} & & & 0 \\ & P_{BN} & & \\ & & P_{NB} & \\ 0 & & & P_{NN} \end{bmatrix}$$

$$\mathbf{M} = \begin{bmatrix} M_{BBBB} & M_{BBBN} & M_{BBNB} & M_{BBNN} \\ M_{BNBB} & M_{BNBN} & M_{BNNB} & M_{BNNN} \\ M_{NBBB} & M_{NBBN} & M_{NBNB} & M_{NBNN} \\ M_{NNBB} & M_{NNBN} & M_{NNNB} & M_{NNNN} \end{bmatrix}$$

$$\mathbf{X} = \begin{bmatrix} X_{BB} & & & 0 \\ & X_{BN} & & \\ & & X_{NB} & \\ 0 & & & X_{NN} \end{bmatrix}$$

When we extend from a one- to a two-dimensional calculation to predict $I(R,Z)$, eq 4 is written in the form of eq 7 as

$$I(R,Z) = \sum_{A} p_A F_{AA}(R,Z) + 2\,\mathrm{Re} \sum_{A}\sum_{B} F_{AB}(R,Z)\, T_{AB}(Z) \quad (9)$$

For the extended random conformation, $F_{AB}(R,Z)$ is given by

$$F_{AB}(R,Z) = \sum_{j}\sum_{k} f_{A,j} f_{B,k} J_0(2\pi R r_{A,j}) J_0(2\pi R r_{B,k}) \exp[2\pi i Z(z_{B,k} - z_{A,j})] \quad (10)$$

and for the extended rigid conformation, the corresponding $F_{AB}(R,Z)$ is given by

$$F_{AB}(R,Z) = \sum_{n}\sum_{j}\sum_{k} f_{A,j} f_{B,k} J_n(2\pi R r_{A,j}) J_n(2\pi R r_{B,k}) \times \exp[2\pi i[(n/2\pi)(\phi_{B,k} - \phi_{A,j}) + Z(z_{B,k} - z_{A,j})]] = \sum_{j}\sum_{k} f_{A,j} f_{B,k} J_0(2R r_{A,j,B,k}) \exp[2\pi i Z(z_{B,k} - z_{A,j})] \quad (11)$$

$r_{A,j,B,k}$ represents the interatomic distance between the jth atom of monomer A and the kth atom of monomer B. The differences between eq 7 and 9 lie in the dimensionality of I and F_{AB}. The paracrystalline lattice defined by $T_{AB}(Z)$ remains the same while the Fourier transforms of the monomer pair convolutions, $F_{AB}(R,Z)$, change with conformation.

Table I
Cylindrical Polar Atomic Coordinates

	r, Å	ϕ, rad	z, Å
HBA			
O_1	0.00	0.00	0.00
C_1	1.14	−1.57	0.77
O_2	2.24	−1.58	0.31
C_2	0.80	−1.54	2.22
C_3	0.73	0.52	2.72
C_4	1.80	−1.91	3.09
C_5	0.88	0.79	4.09
C_6	1.56	−1.97	4.47
C_7	0.28	−1.57	4.97
O_1	0.00	0.00	6.35
HNA			
O_1	0.00	0.00	0.00
C_1	1.25	−1.57	0.56
O_2	2.26	−1.54	−0.09
C_2	1.18	−1.64	2.04
C_3	2.35	−1.88	2.70
C_4	0.44	−0.24	2.78
C_5	2.38	−1.93	4.09
C_6	0.33	−0.29	4.17
C_7	1.20	−1.84	4.83
C_8	1.28	0.86	4.91
C_9	1.23	−1.94	6.22
C_{10}	1.22	0.94	6.31
C_{11}	1.11	−0.74	6.96
O_1'	0.00	0.00	8.37

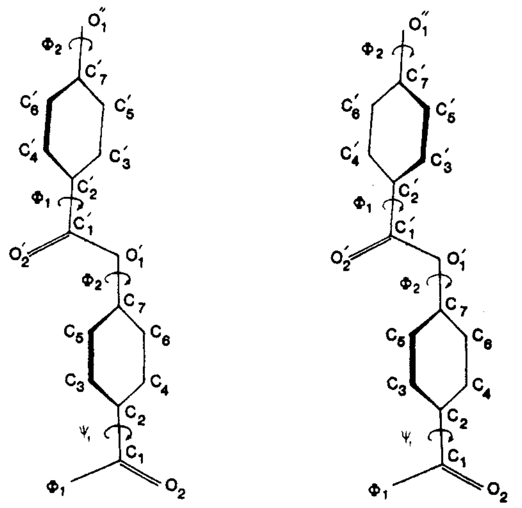

a b

Figure 4. Conformation of the HBA dimer: (a) with parallel aromatic planes and a 2_1 screw axis relating the two monomers; (b) with inclined aromatic planes and a conformation analogous to that in poly(p-phenyleneterephthalamide).

Experimental Section

Table I lists the cylindrical polar coordinates of the HBA and HNA residues, arranged with their terminal ester oxygens on the z-axis. Figure 2 shows these conformations, the numbering of the atoms, and the torsion angles Φ_1 and Φ_2. Φ_1 is set at +30°; $\Phi_1 = 0°$ when $C_1 = O_2$ (carbonyl) is cis to $C_2—C_4$. $I(R,Z)$ was calculated for infinite chains of the two monomers in the random and rigid conformations as defined above. For the rigid conformation, $\Phi_2 = -30°$; $\Phi_2 = 0°$ when C_1'–O_1' (ester) on the next residue is cis to C_7–C_6 (see Figure 4). Models of the chains were also derived as random copolymers of the four possible dimers. This allows us to impose a dimer repeat on the chain, with a

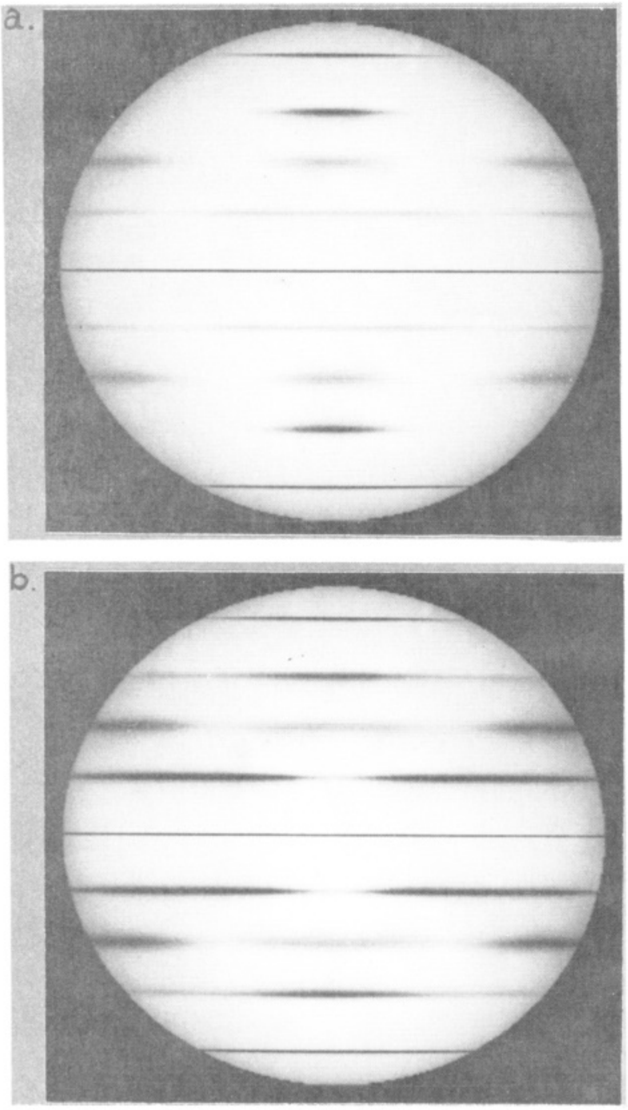

Figure 5. Calculated fiber patterns for infinite chains of 30/70 copoly(HBA/HNA) for (a) an extended random conformation and (b) an extended rigid conformation of the monomers.

specified dimer conformation. Two such conformations were considered: (a) a pseudo 2_1 screw axis in which Φ_1 and Φ_2 assume values of 30° and 150°, respectively, analogous to the proposed structures of poly(HBA)[23] and poly(*p*-benzamide);[24] (b) a conformation analogous to that in poly(*p*-phenyleneterephthalamide),[25] with Φ_1, Φ_2 alternately 30°, 150° and −30°, −150°. Examples of the two types of dimer conformations are shown in Figure 4, which also specifies the aromatic–ester torsion angles.

$I(R,Z)$ was calculated for infinite chains of copoly(HBA/HNA) at mole ratios of 75/25, 58/42, and 30/70. Calculations were done on a 201 × 201 grid along the positive R and Z axes, respectively, but limited to scattering angles of $2\theta \leqslant 50°$ ($\theta = \sin^{-1} [\lambda/2(R^2 + Z^2)^{1/2}]$). The calculated values of $I(R,Z)$ were then put on a scale of 256 shades of grey. A value of 255 (the darkest shade) was assigned to all $I(R,Z)$ values higher than 1500 (normalized to the scattering by one average monomer). This simply truncates the high intensity on the equator and the 2.1-Å layer line, so that the weaker intensities can be observed. Values of $I(R,Z)$ less than 1500 were scaled proportionally. The data were displayed on the monitor of an AED 512 color terminal. All four R,Z quadrants were plotted for comparison with the observed diffraction patterns.

Results and Discussion

Figure 5 shows the calculated intensity for infinite chains of 30/70 copoly(HBA/HNA) for (a) an extended random conformation and (b) an extended rigid conformation, both as defined above. A line of constant intensity (I = 255) was assigned to the equator (Z = 0). Equation 9 predicts infinite intensity in this region, but separate calculations on finite chains show that $I(R,0)$ decreases continuously with increasing R and always exceeds a value of 1500/monomer in the range $2\theta \leqslant 50°$.

Table II
First-Layer Line Data for Copoly(HBA/HNA)

HBA/HNA	R,Z of obsvd off-equatorial, Å^{-1}	calcd Z of first layer line, Å^{-1}
75/25	0.291,0.078	0.079
58/42	0.292,0.072	0.073
30/70	0.294,0.067	0.068

The calculated intensity for the two models consists primarily of a series of layer lines that are extensions of the maxima predicted on the meridian in our earlier work for the one-dimensional case. The intensity agreement on the meridian is to be expected since at R = 0 eq 10 and 11 become identical with each other and with that for the one-dimensional model.[6] The layer line at Z = 1/2.1 Å is the most intense, and high intensity is maintained in the R direction, which is consistent with the observed diffraction data. As discussed previously,[26] the meridional at d = 2.1 Å is a Bragg diffraction maximum that arises due to the fact that the lengths of the HBA and HNA residues are approximately in the ratio 3:4. The sharpness of this layer line in the Z direction is due to the assumption of an infinite straight chain, and it can be broadened by use of a finite chain length or by modeling the nonlinearity of an actual chain conformation.[15]

The major differences between the random and rigid models lie in the relative intensities and extents of the diffuse nonmeridional layer line streaks. In this regard the random conformation shows better agreement with the observed patterns in Figure 1, although it is uncertain how significant this is, given that intermolecular effects have still to be considered. Similar results were obtained for other comonomer ratios. At this point there remains a discrepancy between the observed and calculated intensity data in that there is no obvious intensity maximum predicted in the region where we observe the off-equatorial at d = 3.3 Å, approximately halfway between the equator and the first predicted layer lines in Figure 5a,b.

The R,Z coordinates for the observed off-equatorial maximum are given in Table II for three different compositions. In each case, $1/Z$ is approximately equal to the "average" dimer length for that composition. A layer line at this position cannot occur for the models defined above since each monomer is defined in the same way. To a first approximation we have a "monomer repeat", and the first-layer line spacing corresponds approximately to the average monomer length. To generate a layer line for the observed off-equatorial, there must be some sort of *dimer* repeat unit; i.e., there must be a significant structure difference between adjacent monomers. It should be noted that homopoly(HBA) and poly(*p*-phenyleneterephthalamide) both crystallize with repeats containing two phenylene moieties.[23,25] Three forms of poly(HBA) have been reported,[27] in which the chain has a 2_1 helical conformation with the two HBA residues repeating in 12.6 Å. In poly(*p*-phenyleneterephthalamide), successive phenylene rings are mutually inclined at ~60°, and the repeat is 12.9 Å. In both cases, alternate carbonyl groups point to opposite sides of the chain. Given the similarity of the diffraction data of these homopolymers to those for the copolymers, it is likely that the copoly(HBA/HNA) chain has an analogous pseudodimer repeat. We have considered two conformations: one with a pseudo 2_1 helical structure and one with successive monomers inclined as in poly(*p*-

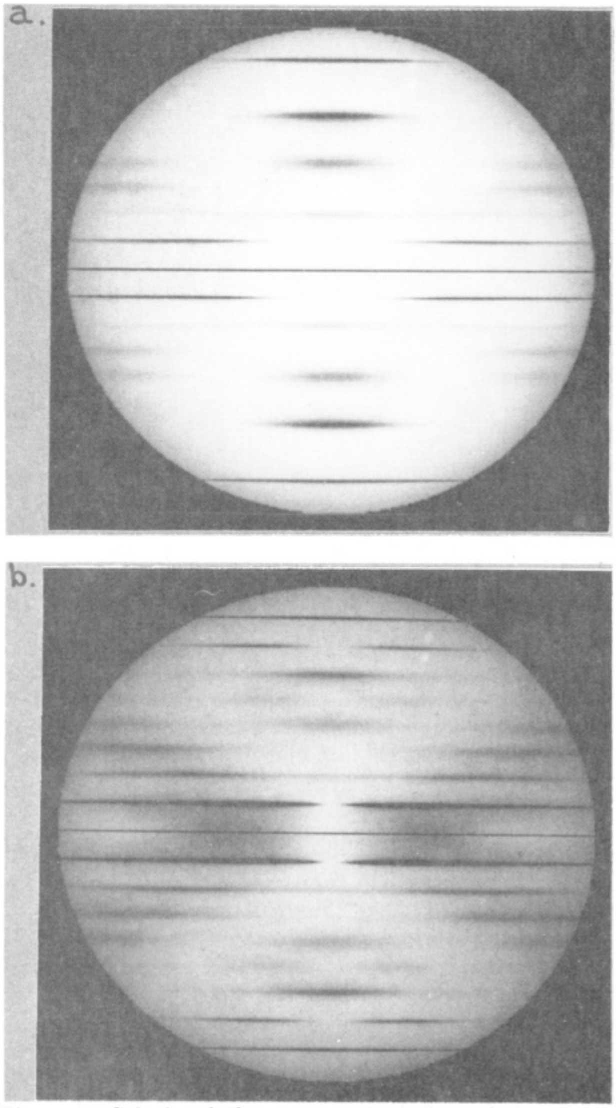

Figure 6. Calculated fiber patterns for infinite chains of 30/70 copoly(HBA/HNA) for (a) a random dimer model and (b) a rigid dimer model. The monomers in the dimer are related by a pseudo 2_1 screw axis.

phenyleneterephthalamide). The torsion angles for these models are given in the Experimental Section. We now extend the concepts of the random and rigid chains to the models built up of dimers and define the "random dimer" model in which there is no rotational correlation between adjacent dimers. Similarly, a "rigid dimer" model is defined in which alternating monomers have the same orientation. In the rigid dimer models constructed from the dimer conformations defined above, the dipoles point toward opposites sides of the chain rather than to the same side as in the rigid monomer model.

Figure 6 shows the calculated intensity transforms for random dimer and rigid dimer models in which the monomers of the dimer are related by a pseudo 2_1 screw axis. The projection of these models onto the z-axis is approximately the same as those for the models considered previously, and hence the predicted meridional intensity is essentially unaffected. However, one can clearly see that the new models generate intensity on a layer line between the equatorial and the first meridional maximum. Calculations done for the other comonomer ratios show that Z for this layer line changes with composition in line with the experimental data. Table II shows that there is agreement within experimental error between the experimental and calculated Z values for the first-layer line for three monomer compositions and that these values correlate approximately with the length of an average dimer. The differences between the intensity transforms for the random and rigid 2_1 dimer models are similar to those between the two monomer models. The rigid model leads to the prediction of more intense off-meridional intensity, as is to be expected in view of the long-term structural correlations. These differences are not large, but it suggests some preference for the randomized model in view of the weakness of the off-meridional intensities in general. It seems likely that there will be more extensive rotational correlations between successive monomers along the chains in the crystalline regions than in the disordered (quenched nematic) regions.

The results obtained using the dimer conformations analogous to that in poly(p-phenyleneterephthalamide) are similar to those in Figure 6 and Table II for the pseudo 2_1 model. The only differences are in the R coordinates of the broad intensity maxima on the layer lines. Both models would give an intense maximum on the first layer line when the molecular transform is sampled by the interference function for the chain packing. Selection between these and other possible chain conformations must be left until we are at the point of refining the three-dimensional model, which will be considered in later papers.

Thus our results point to a chain conformation for copoly(HBA/HNA) in which there is a pseudodimer repeat, which has the attractive feature that successive C=O dipoles point to opposite sides of the chain. These analyses now need to be combined with consideration of interferences due to chain packing.

Acknowledgment. This research was supported by NSF Grant No. DMR 84-17525 from the Polymer Program.

Registry No. (HBA)(HNA) (copolymer), 81843-52-9; HBA (dimer), 40677-31-4.

References and Notes

(1) Calundann, G. W.; Jaffe, M. *Proc. Robert A. Welch Found. Conf. Chem. Res.* **1982**, *26*, 247.
(2) Ba, G. H.; Cluff, E. F. In *Polymeric Liquid Crystals*; Blumstein, A., Ed.; Plenum: New York, 1985; p 217.
(3) Dobb, M. G.; McIntyre, J. E. *Adv. Polym. Sci.* **1984**, *60/61*, 61.
(4) Blackwell, J.; Biswas, A. In *Developments in Oriented Polymers—2*; Ward, I. M., Ed.; Elsevier: Barking, UK, 1987, Chapter 5.
(5) Stamatoff, J. B. *Mol. Cryst. Liq. Cryst.* **1984**, *110*(1–4), 75.
(6) Chivers, R. A.; Blackwell, J.; Gutierrez, G. A. *Polymer* **1984**, *25*, 435.
(7) Gutierrez, G. A.; Blackwell, J.; Chivers, R. A. *Polymer* **1985**, *26*, 348.
(8) Blackwell, J.; Cheng, H.-M.; Biswas, A. *Macromolecules* **1988**, *21*, 39.
(9) Blackwell, J.; Cageao, R. A.; Biswas, A. *Macromolecules* **1987**, *20*, 667.
(10) Calundann, G. W. (Celanese) U.S. Patent 4 161 470, 1979.
(11) Calundann, G. W. (Celanese) U.S. Patent 4 067 852, 1978.
(12) Cottis, S. G.; Economy, J.; Wohrser, L. (Carborundum) U.S. Patent 3 975 487, 1976.
(13) Osawa, S.; Nakagawa, Y.; Matsuda, K.; Nishihara, T.; Yuroki, H. Japan Patent Doc 52-39719, 1952, 53-32838, 1953.
(14) Blackwell, J.; Gutierrez, G. A.; Chivers, R. A. *Macromolecules* **1984**, *17*, 1219.
(15) Biswas, A.; Blackwell, J. *Macromolecules*, companion papers in this issue.
(16) Windle, A. H.; Viney, C.; Golombok, R.; Donald, A. M.; Mitchell, G. R. *Faraday Discuss. Chem. Soc.* **1985**, *No. 79*, 55.
(17) Butzbach, G. D.; Wendorff, J. H.; Zimmermann, H. J. *Polymer* **1986**, *27*, 1337.
(18) Cao, M. Y.; Wunderlich, B. *J. Polym. Sci., Polym. Phys. Ed.* **1985**, *23*, 521.
(19) Clements, J.; Humphrey, J.; Ward, I. M. *J. Polym. Sci., Polym. Phys. Ed.* **1986**, *24*, 2293.
(20) Blundell, D. J.; Buckingham, K. A. *Polymer* **1985**, *26*, 1623.

(21) Chivers, R. A.; Blackwell, J. *Polymer* **1985**, *26*, 997.
(22) Bonart, R. C.; Blackwell, J.; Biswas, A. *Makromol. Chem., Rapid Commun.* **1985**, *6*, 353.
(23) Geiss, R. H.; Street, G. B.; Volksen, W.; Economy, J. *IBM J. Res. Dev.* **1983**, *27*(4), 321.
(24) Tadokoro, H. *Structure of Crystalline Polymers*; Wiley: New York, 1979; Chapter 7.
(25) Northolt, M. S. *Eur. Polym. J.* **1974**, *10*, 799.
(26) Blackwell, J.; Biswas, A.; Gutierrez, G. A.; Chivers, R. A. *Faraday Discuss. Chem. Soc.* **1985**, *No. 79*, 73.
(27) Blackwell, J.; Lieser, G.; Gutierrez, G. A. *Macromolecules* **1983**, *16*, 1418.

Three-Dimensional Structure of Main-Chain Liquid-Crystalline Copolymers. 2. Interchain Interference Effects

Amit Biswas and John Blackwell*

Department of Macromolecular Science, Case Western Reserve University, Cleveland, Ohio 44106-2699. *Received December 7, 1987*

ABSTRACT: Previous analyses of the X-ray fiber diagrams of wholly aromatic copolyesters have shown that these systems consist of oriented arrays of chains with completely random comonomer sequence. Nevertheless, these copolymers exhibit sharp equatorial and off-equatorial Bragg maxima that are indicative of three-dimensional crystallinity. This paper shows that these diffraction characteristics are predicted when limited register occurs between adjacent chains. This is achieved when one monomer on each chain of the array comes into register in a plane perpendicular to the fiber (chain) axis. As such, this requires a small shift for each chain (~4 Å at the most) from the arrangement in a nematic structure. Analyses are developed to predict the interference effects for three-dimensional arrays of copolymer chains, with or without chain register. The results show that in as-spun fibers even the limited register described above exceeds that necessary to generate the observed diffraction effects. Rather, there is a normal distribution of chain origins about the registry plane, with a standard deviation of ~2 Å, which corresponds to only a small preference for registration.

Introduction

The X-ray data for thermotropic wholly aromatic copolyesters are very intriguing because these polymers exhibit substantial three-dimensional crystallinity despite the fact that they have a random comonomer sequence. The latter fact has been established by X-ray analyses in this and other laboratories over the last few years.[1-4] The X-ray fiber diagrams contain a series of aperiodic meridional maxima, and it has been shown that these are reproduced in position and approximate intensity in theoretical calculations for nematic arrays of extended chains of completely random sequence.[5,6] When nonrandom sequence distributions are considered by variation of nearest-neighbor statistics, the agreement between the observed and calculated meridional data becomes unacceptable for all but minimal blockiness.[7,8]

The evidence for three-dimensional order comes from the presence of sharp equatorial and off-equatorial Bragg reflections in the fiber diagrams. Three-dimensional register is required by the presence of a sharp off-equatorial at $d \cong 3.3$ Å, which occurs at a layer line spacing of 12–15 Å, depending on the chemical composition. Thermal annealing of these copolymers can result in a sharpening of these reflections corresponding to an increase in crystallite size,[9] and there can be the generation of additional maxima, some of which may be due to development of an additional polymorphic structure.[10] Application of the Scherrer equation to the equatorial maxima yields crystallite widths of 70–190 Å,[11] depending on the thermal history, which indicates large ordered regions consisting of ~200–1500 chains. In addition, degrees of crystallinity as high as 80% have been reported,[12] based on division of the diffraction data into "crystalline" and "amorphous" components. Typical values for quenched specimens are in the range 30–50%, which increases on annealing.[13] It should be noted that annealing does not lead to changes in the positions of the meridional maxima; i.e., there is no evidence for any departure from a random sequence distribution.[10]

Our previous analyses of the structure addressed a one-dimensional problem, since the diffraction along the meridian is derived from the projection of the "average" chain onto the fiber axis. In view of the approximate linearity of the chain, this projection is approximately independent of conformation. However, when we attempt to derive a three-dimensional structure from the entire diffraction pattern, it is necessary to consider the actual chain conformation. Our first step in analyzing the structure was to calculate the cylindrically averaged transform for individual chains of average sequence. The original approach described by Chivers and Blackwell[14] for the copolyester of *p*-hydroxybenzoic acid (HBA) and 2-hydroxy-6-naphthoic acid (HNA) has been generalized for other chemical structures and applied to different conformations.[15] The main conclusion is that the chains have a pseudo "dimer repeat", with the successive ester groups pointed to opposite sides of the chain, analogous to the dimer repeats observed for homopoly(HBA)[16] and poly(*p*-phenyleneterephthalamide).[17] This pseudo dimer repeat is necessary, since correlations between successive monomers in the dimer are responsible for the generation of the layer line on which the off-equatorial maximum lies.

The present paper considers the interference effects that occur when these chains are packed with their origins on a two-dimensional network. If the origin atoms are coplanar but there is no radial correlation for the chain position, i.e., there is cylindrical averaging of the chains independent of the two-dimensional lattice, then the effect of interference is to sample the cylindrically averaged transform for the chain at the lattice points. The fact that layer line reflections are observed in the fiber diagrams means that we must have some sort of chain register. Such register is likely to involve stacking of aromatic groups or dipole–dipole interaction of the carboxyl groups, and hence there will be a spatial correlation between certain monomers on adjacent chains.

The first possibility for chain register that comes to mind is the lateral alignment of homopolymer sequences, some

0024-9297/88/2221-3152$01.50/0